

**Report on the expected PGV and PGA values for induced
earthquakes in the Groningen area**

Bernard Dost, Mauro Caccavale, Torild van Eck, Dirk Kraaijpoel

**KNMI
December 2013**

Summary

Recent developments in the analysis of seismic activity of the Groningen gas field showed that the estimated maximum magnitude for induced events in the region can be higher than previously thought ($M_{\max} > 3.9$). A preliminary new value for the M_{\max} was estimated at $M=5$. This report presents the results of an analysis of the expected peak ground velocities (PGVs) and peak ground accelerations (PGAs) assuming a maximum magnitude $M=5$.

Selection of the most appropriate ground motion prediction equation (GMPE) for the Groningen area is a key issue in the analysis. Since there is no known natural seismicity in the region and recorded induced seismicity is limited to $M \leq 3.6$, relations based on shallow earthquakes from other regions have been evaluated. The selected GMPE, based on shallow earthquakes from Europe and the Middle-East, has been modified to fit recorded PGAs and PGVs in Groningen for 8 induced events and was adopted as a reference model for Groningen. The model includes a correction factor for a shallow low velocity layer, which is present in the region.

Based on this new GMPE for Groningen and a selection of the source region, deterministic scenario's are calculated for a $M=5$ event. The source region was selected based on the occurrence of previous events with $M \geq 3$ and contours of the highest median PGV and PGA are presented. The highest median value for PGV is 10.5 cm/s and for PGA 0.2g.

In addition, a probabilistic seismic hazard analysis (PSHA) was carried out. Induced seismicity in Groningen shows a time varying pattern and increases with increasing production. This non-stationary character has been taken into account by estimating the increase in seismicity rate for the next five years, since there is no resolved change in the b-value of the Gutenberg-Richter relation for the region over time. The maximum magnitude is one of the parameters in the PSHA. A re-evaluation of the estimation of this parameter for Groningen did not result in a reliable new value, so $M_{\max}=5$ was used in the analysis. Results are shown as PGA and PGV contours for a 10% probability of exceedance in 50 years. The maximum PGA value is 0.42g and the maximum PGV is 16 cm/s.

Uncertainties in the parameters used in the PSHA are high and this results in a possible overestimation of the hazard. Further research is focused on reducing the uncertainties in these parameters.

Introduction

The largest recorded induced earthquake in the Netherlands, $M_w = 3.6$, occurred August 16, 2012 near Huizinge in the province of Groningen at a depth of 3 km. This event caused over 3000 damage claims in the region and a re-assessment of the seismic hazard for the region was made based on recorded induced seismicity data up to September 2012 (Dost and Kraaijpoel, 2013; Muntendam and de Waal, 2013). One of the conclusions was that the maximum probable magnitude (M_{max}) for the Groningen field could not be reliably assessed from the data. Due to the sparse dataset, previous estimates of M_{max} were based on seismicity data for all gas producing fields in the Netherlands together. Comparison with induced seismicity in other hydrocarbon fields in the world led to the conclusion that M_{max} was not expected to exceed a magnitude 5. The current report investigates the expected ground motion in the Groningen area due to a magnitude 5 earthquake.

As a first step, the most appropriate Ground Motion Prediction Equation (GMPE) will be selected. A GMPE relates magnitudes to peak ground velocities (PGV) and peak ground acceleration (PGA) and forms one of the basic building blocks in seismic hazard calculations. Existing GMPEs are usually constructed for earthquakes of magnitude larger than 5, while in the Groningen area we have measured PGV and PGA values only for events of $M \leq 3.6$. Extrapolation from large to small earthquakes, using empirical GMPEs, have the tendency to overestimate the PGA and PGV values (Bommer et al., 2007), which was also concluded in the derivation of an attenuation relation for shallow events in the Netherlands (Dost et al., 2004).

A second step is the selection of the source area where a magnitude 5 earthquake can be expected. The driving force behind the occurrence of hydrocarbon induced seismicity is thought to be (differential) compaction of the reservoir (e.g. Dost and Haak, 2007). In addition Van Eijs et al. (2006) found that fault density and the ratio in Young's moduli between overburden and reservoir are key indicators for the occurrence of seismicity in the gas fields in the Netherlands. This implies that compaction, fault density and the ratio of the Young's moduli play an important role in the definition of the source region.

In addition to a deterministic scenario for a magnitude 5 earthquake, also results from a probabilistic hazard analysis will be included. These results are presented in terms of a 10% probability in 50 years to exceed PGA and PGV values, or its equivalent a return period of 475 years.

The last step to convert the PGA or PGV values for Groningen into Intensities has not been carried out in this report. Existing relations developed for other regions have been evaluated. Since this conversion adds a very large uncertainty and there is an urgent need to have PGA and PGV estimates as input for other research topics (e.g. quick-scan), this report will be limited to a presentation of contour plots of the expected PGA and PGV values.

Ground Motion Prediction Equations (GMPEs)

In the Groningen area a rather limited dataset is available of recorded (peak) ground motions for magnitudes $M \leq 3.6$. No reliable local ground motion measurements are available to constrain the ground motion for $M > 3.6$ and therefore empirical GMPEs are evaluated based on data from other seismic areas with some similarity to our local situation.

Bommer (2013a) compiled a set of GMPEs that may be relevant for the Groningen region and presented a revised set of selection criteria with respect to earlier work on this topic (Bommer et al., 2010). The focus is on horizontal components of motion.

Important criteria are:

- Magnitude range used
- Horizontal component definition
- Magnitude scale
- Distance metric
- Site classification

Since this research is focused on shallow events, < 5 km depth, of magnitude $3.5 < M < 5$, GMPEs should preferably include at least this magnitude range. Although recently there is a tendency to include smaller magnitudes in the GMPEs, application of this criterion alone limits the number of available models to 16 (Bommer 2013a). Although in general the geometric mean of the two horizontal components is used in the definition of the PGA and PGV values, some models use the larger component or even the largest of three components. A number of GMPEs do not specify which definition of the horizontal component was used, thus adding a degree of uncertainty since different definitions can yield peak motions varying by 10-15% (Beyer & Bommer, 2006). As a distance metric the hypocentral distance (R_{hyp}) is preferred, which means that earthquakes are regarded as point sources. This is in line with the requirements of initial hazard models based on the selected GMPE. Bommer et al. (2012) show that the key issue in seismic hazard analysis is consistency between the distance metric in the GMPE and the way earthquakes are represented in the seismicity model. In addition Bommer et al. (2010) mention that the use of R_{hyp} as distance metric becomes inappropriate for larger earthquakes associated with fault ruptures of tens or even hundreds of kilometres in length. Most important in the selection was the issue of site classification. Models based on only a limited number of site classes were rejected, since they are difficult to adopt for the northern Netherlands. Also, models only predicting motions on hard rock sites were rejected.

Especially the last criterion reduced the total number of models to the Chiou et al. (2010) model (C10) and the Dost et al. (2004) model (D04). Since the C10 model uses a different distance metric, R_{rup} , being the distance to the closest point on the rupture plane, which is difficult to estimate for larger recorded events in the Groningen field, it was decided to use the D04 model in initial hazard calculations. Rupture dimensions of the larger recorded events are small enough for R_{hyp} to be used as a surrogate. However, for extrapolation to higher magnitudes the D04 model does not include an appropriate non-linear scaling effect and will, most likely, overestimate PGV and PGA. Bommer (2013a) proposed to modify D04 to include this non-linear scaling following a newly developed model for Europe and the Middle East (Akkar et al., 2013), based on shallow earthquakes and includes short distances. This last model is based on a magnitude range $4 < M_w < 7.6$, is developed for the geometric mean of the horizontal components and for different distance metrics, including R_{hyp} . In addition it has a similar site classification as the C10 model and qualifies as an additional model in this analysis.

In the construction of a general GMPE for induced seismicity in geothermal areas, Douglas et al. (2013) used data from the Roswinkel gas field, a small field south-east of the Groningen field, combined with acceleration data from other sources of induced seismicity in very different tectonic environments. They produce two types of models: uncorrected and corrected for site effects. The uncorrected model provides an average value over a large variation of shallow structure. As a consequence the variance is large. The corrected version will need the addition of shallow structure, which means that site amplification effects need to be added, since the adjusted Douglas et al. (2013) equations are referenced to hard rock sites ($V_{s30} > 1$ km/s). This information is not available for Groningen. Therefore, it was decided not to use this model, which was also recommended by Bommer (2013a).

Based on these considerations, two models have been selected: the local model by Dost et al. (2004), referred to as D04, and the European model of Akkar et al. (2013), referred to as ASB.

Model characteristics

D04

This model is partly based on measured accelerations near the Roswinkel gas field and on an attenuation relation calculated for the determination of M_L using the regional borehole network in the north of the Netherlands (Dost and Haak, 2007). The distance metric is R_{hyp} , the definition of horizontal components is the geometric mean of the rotated components and for the magnitude M_L was selected, assuming an equivalence of M_L and M_w for the small magnitudes ($M \leq 3.9$) used.

The relation for PGV is:

$$\log(PGV) = -1.53 + 0.74M_w - 0.00139R_{hyp} - 1.33 \log(R_{hyp}) + \epsilon \sigma \quad [1]$$

PGV in cm/s and R_{hyp} measured in km, ϵ is the standard normalised residual and σ is the standard deviation. The D04 model shows a linear dependence on magnitude. Since most models based on larger magnitude events show a saturation of the PGV levels, Bommer (2013) proposed a modification of the D04 model. This modification was constructed by comparison with the ASB model. For $M \geq 4.5$, equation [1] is replaced by:

$$\log(PGV) = -1.3972 + 0.7105M_w - 0.0829(M_w - 4.5)^2 - 0.00139R_{hyp} - 1.33 \log(R_{hyp}) + \epsilon \sigma \quad [2]$$

The relation for PGA is:

$$\log(PGA) = -1.41 + 0.57M_w - 0.00139R_{hyp} - 1.33 \log(R_{hyp}) + \epsilon \sigma \quad [3]$$

PGA in m/s^2 . Modified along similar lines as for PGV (pers. comm., Bommer, 2013):

$$\log(PGA) = -1.609 + 0.614M_w - 0.1116(M - 4.5)^2 - 0.00139R_{hyp} - 1.33 \log(R_{hyp}) + \epsilon \sigma \quad [4]$$

Standard deviation for both relations is $\sigma = 0.33$. Since most other relations are in the natural logarithm (ln), the equivalent in ln is equal to $\sigma/\log(e) = 0.76$.

ASB

This model is the latest generation ground motion models based on pan-European databases. The model includes a non-linear site amplification function that is a function of V_{s30} and is based on a dataset containing events with a minimum magnitude of $M_w=4$. All earthquakes in the database used are shallower than 30 km and 20 events have a depth shallower than 5 km and a normal faulting mechanism, which is the assumed dominant mechanism in Groningen. The model is developed for a number of distance metrics (R_{epi} , R_{hyp} , R_{jb}) and uses the geometric mean of the unrotated horizontal components.

The equation used is:

$$\ln(X) = \ln(X_{REF}) + \ln(S) + \epsilon\sigma \quad [5]$$

where X can be PGV or PGA and

$$\ln(PGV_{REF}) = 6.72743 + 0.0029(M_w - 6.75) - 0.11474(8.5 - M_w)^2 + [-1.17694 + 0.2529(M_w - 6.75)] \ln(\sqrt{R^2 + 7.5^2}) - 0.0616F_N + 0.063 \quad [6]$$

$$\ln(S) = -0.72057 \ln\left(\frac{V_{S30}}{V_{REF}}\right) - 0.19688 \ln\left(\frac{PGA_{REF} + 2.5\left(\frac{V_{S30}}{V_{REF}}\right)^{3.2}}{(PGA_{REF} + 2.5)\left(\frac{V_{S30}}{V_{REF}}\right)^{3.2}}\right) \quad [7]$$

PGA_{REF} is calculated using

$$\ln(PGA_{REF}) = 3.26685 + 0.0029(M_w - 6.75) - 0.04846(8.5 - M_w)^2 + [-1.47905 + 0.2529(M_w - 6.75)] \ln(\sqrt{R^2 + 7.5^2}) - 0.1091F_N + 0.0937F_R \quad [8]$$

$$\ln(S) = -0.41997 \ln\left(\frac{V_{S30}}{V_{REF}}\right) - 0.28846 \ln\left(\frac{PGA_{REF} + 2.5\left(\frac{V_{S30}}{V_{REF}}\right)^{3.2}}{(PGA_{REF} + 2.5)\left(\frac{V_{S30}}{V_{REF}}\right)^{3.2}}\right) \quad [9]$$

In these equations R is the hypocentral distance, F_N and F_R are unity for normal and reverse faults respectively. The V_{REF} is defined at 750 m/s and the average V_{s30} for Groningen is around 200-300 m/s. The variance is specified for PGV ($\sigma=0.71$) and for PGA ($\sigma=0.7347$). The units of the predicted quantities are [g] for PGA and [cm/s] for PGV.

Magnitudes

Local magnitudes (M_L) of induced earthquakes in the Netherlands are calculated using an empirical attenuation function, derived on the basis of Wood-Anderson simulated recordings of 200m deep borehole sensors in the region (Dost et al., 2004). In the GMPEs both M_w and M_L are used and for small events, $3 < M < 5$, it is assumed that $M_L = M_w$ (Hanks and Boore, 1984; Deichmann, 2006). The latter showed that for $M_w < 2$, M_L is expected to be systematically underestimated.

Bommer (2013a) discussed this issue in relation to the Douglas et al (2013) findings that for Roswinkel data a relation between both magnitudes was developed: $M_w = 0.578 * M_L + 1.168$, based on measured M_w values using an automated procedure. Although in this procedure the regional very low Q values ($20 < Q < 80$) and high values for the site attenuation factor ($0.02 < \kappa < 0.05$) have not been taken into account, the outcome inspired to process the available data for Groningen.

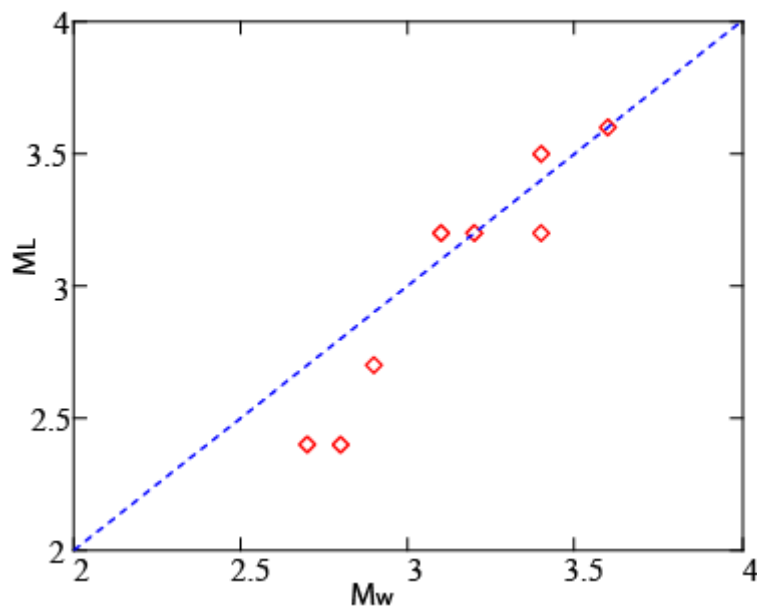


Figure 1 . Comparison of measured M_w and M_L data for events located in the Groningen field

Figure 1 plots the results, using the same model parameters as in Dost and Kraaijpoel (2013). Results seem to corroborate the findings of Hanks and Boore (1984), although the dataset needs to be enlarged. Bommer (2013a) investigated the effect of the magnitude conversion proposed for the larger magnitudes, but concluded this would lead to unrealistic PGV values. It should be noted that the D04 model does not include saturation for the larger magnitudes.

Horizontal component definition

The D04 model is based on the geometric mean of the rotated components of measured accelerations. Other models, including the ASB model, use the unrotated components. Although the difference may not be very large, we investigate the difference for the measured accelerations of the Huizinge event.

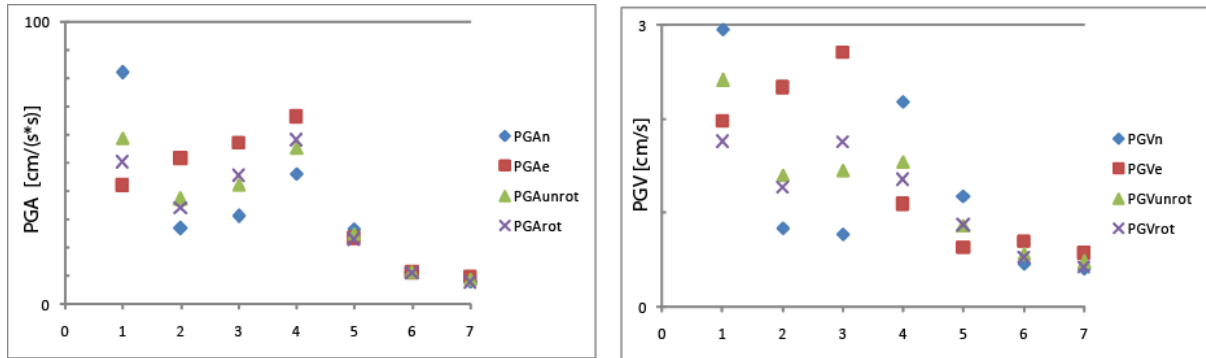


Figure 2. Left: Unrotated (PGAunrot) and rotated (PGArrot) PGA geometrical mean values, compared with the original unrotated PGA measurements. Right: same for PGV.

From the left panel in Figure 2 it is clear that there is a difference in PGA, especially for the larger values. For this event the maximum difference in PGA is 17% and this should be taken into account. The same for PGV shows a similar result with even larger difference up to 37% for the largest motion. This was recorded in station Middelstum-1 (MID1) at a hypocentral distance of 3.2 km. Due to a highly polarized signal, the geometric mean of the two rotated components gives a smaller value than the original measured NS and EW components.

Decomposition of the standard deviation

Bommer (2013a) discusses the necessity to decompose the standard deviation in the GMPEs into an inter- and intra-event (or between- and within-event) component, a requirement when calculating the hazard – and risk- at multiple locations simultaneously. The between-event component (τ) reflects differences in source features, while the within-event component (ϕ) reflects azimuthal differences in radiation pattern, travel path and subsurface structure.

The D04 model only delivers a total standard deviation and Bommer (2013a) proposes to use a ratio $\phi/\tau = 2$, based on a comparison with other published models. This leads to:

$$\tau = 0.1476 \quad \text{and} \quad \phi = 0.2952 \quad \text{and} \quad \sigma = \sqrt{\tau^2 + \phi^2},$$

where σ is the standard deviation of $\log(\text{PGV})$. The same is valid for $\log(\text{PGA})$. For $\ln(\text{PGV})$ the values are: $\tau = 0.3399$ and $\phi = 0.6798$ ($\sigma = 0.76$)

In the ASB model the total standard deviation is decomposed in terms of τ and ϕ :

For $\ln(\text{PGV})$: $\tau = 0.3312$ and $\phi = 0.6280$ ($\sigma = 0.71$)
 For $\ln(\text{PGA})$: $\tau = 0.3472$ and $\phi = 0.6475$ ($\sigma = 0.7347$)

Model validation - PGV

Both remaining GMPEs are dependent on hypocentral distance and magnitude. First their relation with hypocentral distance is investigated. Figure 3 shows both models for two selected magnitudes: $M_w=3.5$ can be compared to measured accelerations in the region (validation) and $M_w=5.0$ is the target magnitude. Both the median value and the median $\pm\sigma$, the standard deviation, are shown for each model. Results are shown for the uncorrected version of the D04 model.

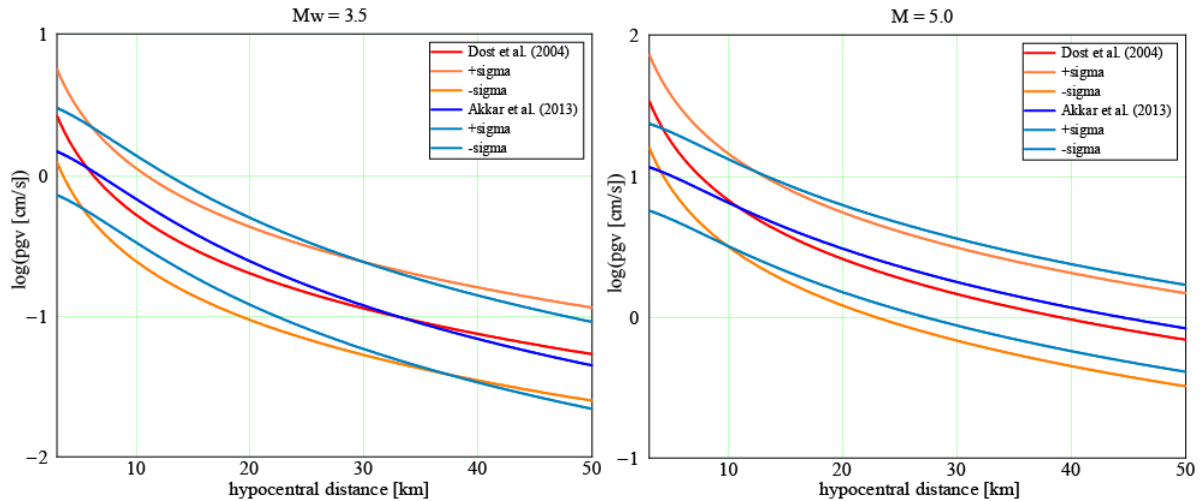


Figure 3. Log(PGV) as a function of hypocentral distance for two selected models (D04 and ASB) for $M_w=3.5$ (left) and $M_w= 5.0$ (right). Models are shown including their standard deviation σ .

Both models are comparable and start to deviate for small hypocentral distances. For $M_w=5.0$ the differences are pronounced for $R<10$ km, while for $M_w=3.5$ this distance is reduced to $R<5$ km.

Important in the evaluation of these GMPEs is the calibration with existing data. In Figure 4 both models are shown together with the PGV data from the 2012 Huizinge event. In Dost and Kraaijpoel (2013) the values for the epicentral distance are given with respect to the original location based on the borehole data and only arithmetic mean values are listed. In Table 1, we give updated values with respect to the final epicentre and provide geometrical mean values for PGA and PGV values. Please note that data from station FRB2 are not included due to suspected malfunctioning of the instrument.

Station	PGAr hor. [cm/s ²]	PGVr hor. [cm/s]	PGA [cm/s ²]	PGV [cm/s]	Epic dist. [km]	Hypoc. dist. [km]
MID1	50.5	1.76	58.8	2.41	1.2	3.2
KANT	34.2	1.28	37.3	1.40	2.7	4.0
WSE	45.6	1.76	42.4	1.45	3.7	4.8
GARST	58.3	1.36	55.5	1.55	4.1	5.1
STDm	22.9	0.87	25.1	0.86	5.2	6.0
WIN	11.0	0.52	11.4	0.57	7.6	8.2
HKS	7.8	0.43	8.8	0.48	11.0	11.4

Table 1. Measured geometric mean horizontal values of PGA and PGV for the 120816 Huizinge event. Both the rotated (PGXr) and unrotated (PGX) values are given, where X equals A or V.

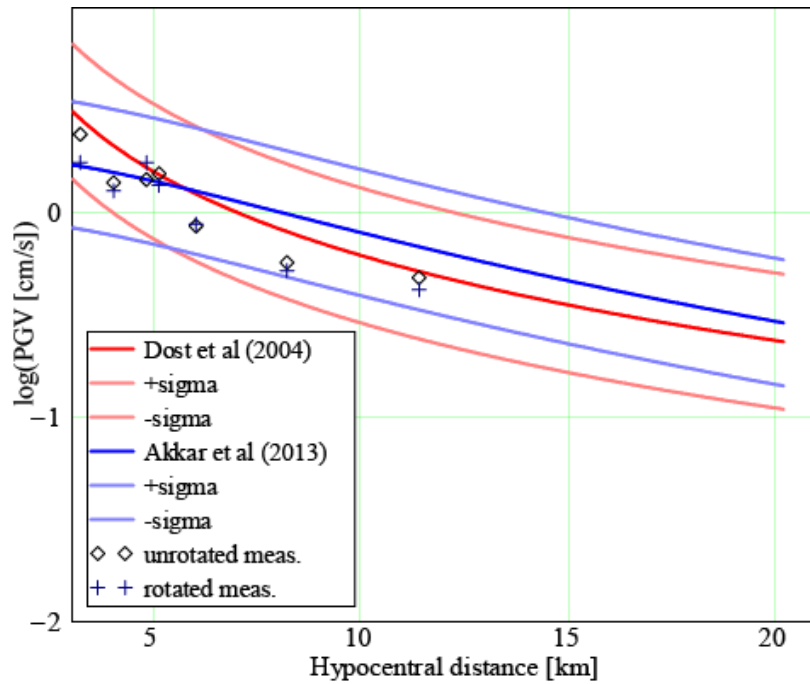


Figure 4. Log(PGV) as a function of hypocentral distance for selected models compared to measured values of the 120816 Huizinge event. Both unrotated and rotated measurements are shown.

Although the measurements in Figure 4 do not seem to support the large increase in PGV at $R < 5\text{ km}$ in the D04 model, this should be investigated using a larger dataset. Since the D04 model is based on polarized recordings, polarized (rotated) measurements (+) should be compared to the model output, while unpolarized data should be compared to the ASB model.

In Figure 5 both models are compared with respect to their magnitude dependence. The effect of the linear dependence of magnitude in D04 is clearly seen at the high magnitude level. Differences between the GMPEs are mainly restricted to the lower values of R .

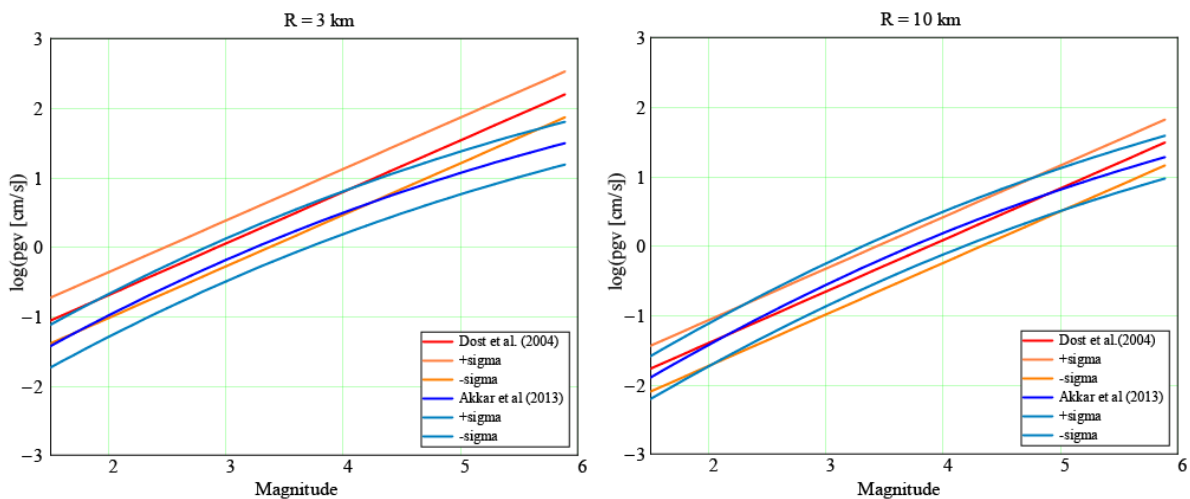


Figure 5. Comparison of the selected GMPEs (D04 and ASB) as a function of magnitude for $R=3\text{ km}$ (left) and $R=10\text{ km}$ (right).

Model validation - PGA

Similar to the PGV calculations, Figure 6 shows the relation between PGA and hypocentral distance for selected magnitudes.

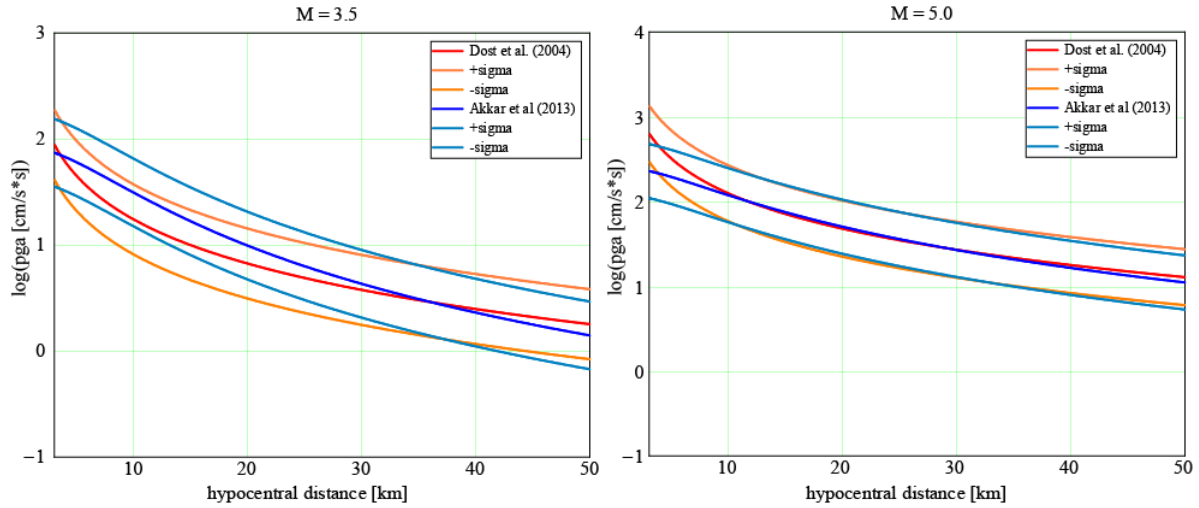


Figure 6. Log(PGA) as a function of hypocentral distance for two selected models (D04 and ASB) for $M_w=3.5$ (left) and $M_w=5.0$ (right).

For the low magnitude $M_w=3.5$, the amplitude attenuation with distance is much more pronounced in the PGA case, compared to the PGV. For $M_w=5.0$ both models provide similar output, except for the short distances ($R < 10$ km).

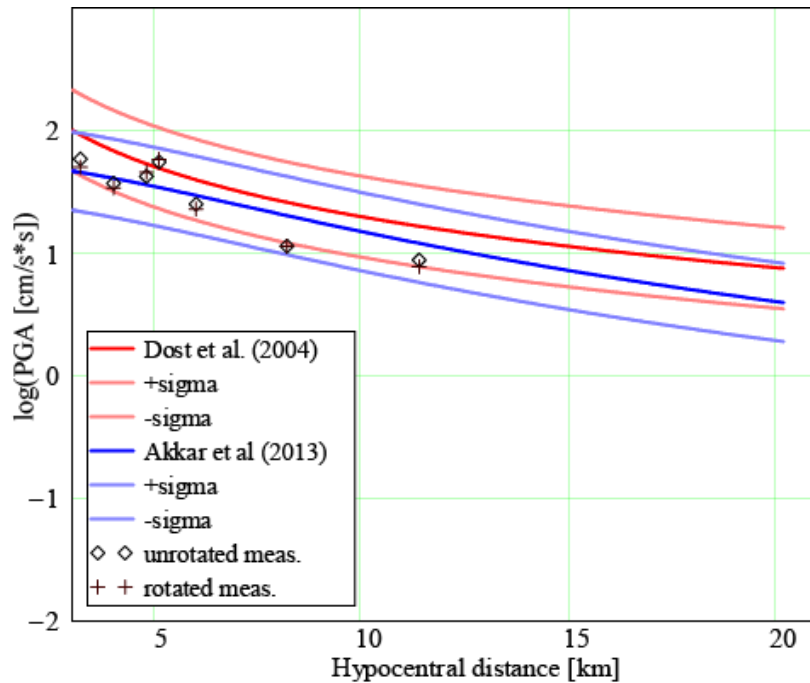


Figure 7. Measured acceleration data (PGA) from the Huizinge event compared to models D04 and ASB. For the ASB model $V_{s30}=200$ m/s is used.

Figure 7 shows the fit of the measured accelerations to the selected models. Similar to the conclusions for PGV, the PGA measurements do fit both models reasonably well. As discussed before, there is less difference between the polarized and unpolarized measurements and there is no indication for a strong increase in PGA or PGV at small values of R.

Comparison of both D04 and ASB with existing acceleration data for Groningen shows that the ASB model is the preferred starting model for hazard calculations. Both D04 and ASB models fit the data reasonably well, but there are two main problems with the D04 model. Due to the availability of data from only small magnitude events D04 cannot be used to provide reliable estimates of PGV and PGA for larger events, although modifications based on the ASB model are proposed by Bommer (2013b) to overcome this problem. The second issue is the large increase of the PGV and PGA value at short distances, which is regarded as unrealistic (Bommer, 2013b). Comparison with the data from the Huizinge event showed that there is no need to include such an increase to explain the data. In addition Korff et al. (2013) showed that the recorded acceleration spectra in Groningen fit well with the predicted values using the ASB model. Thus suggesting that shallow induced events can be modelled similar to tectonic events.

An extension of the acceleration database was prepared, consisting of recordings from seven other events that occurred in the Groningen field. Bommer (2013b) evaluated the dataset, found that a] the ASB model overestimates the PGA and PGV measurements and b] the model shows a trend with magnitude and proposed a modification to the model to fit the data. For events of $M_w \leq 4.2$ the modification for PGA is:

$$\ln(PGA_{REF}) = -3.161825 + 1.5029M_w - 0.04846(8.5 - M_w)^2 + [0.55634M_w - 4.460575] \ln\left(\sqrt{R^2 + (2.593M_w - 3.389)^2}\right) \quad [10]$$

For PGV the threshold magnitude is M_w 3.8 and the modification:

$$\ln(PGV_{REF}) = 1.136255 + 1.4529M_w - 0.11474(8.5 - M_w)^2 + [0.480586M_w - 3.749226] \ln\left(\sqrt{R^2 + (3.043M_w - 4.065)^2}\right) \quad [11]$$

The residuals of the Groningen data with respect to the proposed modifications are small and do not show significant trends with distance or magnitude. In addition the relations for the higher magnitudes did not change. The estimated variance in both modified relations is $\sigma = 0.4$. These modified relations are preferred for hazard assessment. It should be kept in mind that the PGA and PGV values for magnitudes larger than the thresholds mentioned are not constrained by any data from Groningen or the Netherlands. The dataset used to construct the ASB model includes shallow events and V_{s30} values comparable to measured V_{s30} in Groningen and is therefore assumed to be representative for Groningen.

Deterministic PGV and PGA contours for Groningen

For the construction of a PGV or PGA contour map in the Groningen area due to an $M_w=5$ in the region, a selection of the source region should be made. Different options are considered, assuming only an $M=5$ event will be generated:

- along one of the larger faults systems in the region that are known from 3D seismics. The source region could be defined by mapped faults that have shown to be re-activated.
- at a threshold level of compaction
- at locations where in the past $M \geq 3.0$ earthquakes have been recorded

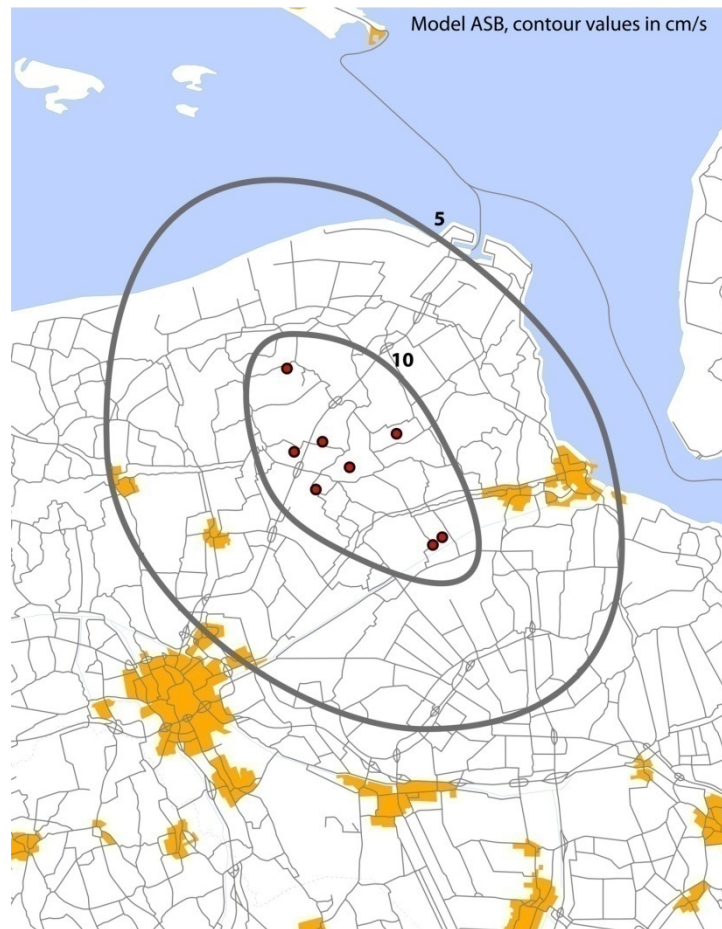
The first option could be considered, since larger fault systems in the region are mapped. However, the location of the induced earthquakes has limited accuracy in the horizontal plane (0.5-1 km) and around 2 km in the vertical plane, due to the existing sparse network in the region. The seismicity patterns seem to line up with existing faults, but this cannot be quantified and fault re-activation studies are being carried out at this moment. The empirical relationship of Wells & Coppersmith (1994; Table 2A), relating subsurface rupture length to magnitude, suggests that an $M=5$ earthquake would only require a total rupture length of 3.2 km. However, for shallow earthquakes in weak sediments the shear modulus is small and therefore a given seismic moment is reached by either larger slip or a larger source area (e.g. Cesca et al., 2011)

The second option to use the compaction model of the Groningen field and impose a minimum level of compaction needed to create larger events is a valid alternative. However, since Van Eijs et al. (2006) showed a correlation between fault density and seismicity, it is recommended to combine both compaction and fault density or the existence of large faults.

In this report we selected the third option as a starting point, mainly because of limitations in applying either of the other two, which may be updated if more information is available to use either of the two other options. There is an implicit assumption that the spatial distribution of earthquakes is stationary in time.

Deterministic PGV contour

Figure 7 shows the contours of the highest median PGV value due to any $M=5$ earthquake in the area spanned by the historic $M \geq 3$ earthquakes. Although an unrealistic scenario, it provides an overview in one Figure. An alternative is to provide a separate figure for each possible source.



Figuur 7. Contours for the highest median PGV due to a $M_w=5$ event in the area spanned by the location of historical $M \geq 3$ events. Seismic sources are indicated as red circles, contours as grey lines. Median values are shown in cm/s.

The figure was constructed by calculating the radius of the selected contours, using the ASB model, applying circles with this radius to all seismic sources and to contour the envelope of the combined set of circles.

The contours are based entirely on median predictions from the model equations. Addition of one standard deviation provides approximately a factor two increase in the PGV and PGA values. The maximum PGV value in Figure 7 is 10.5 cm/s. Lower and upper limits for the maximum PGV (median $\pm \sigma$) are: 5.2 cm/s and 21.3 cm/s.

Deterministic PGA contour

Figure 8 shows similar contours for PGA. Values are given in $[g]^1$ instead of cm/s^2 , which was used in the rest of the text. This was requested by other research groups that will be using these preliminary results in their study.

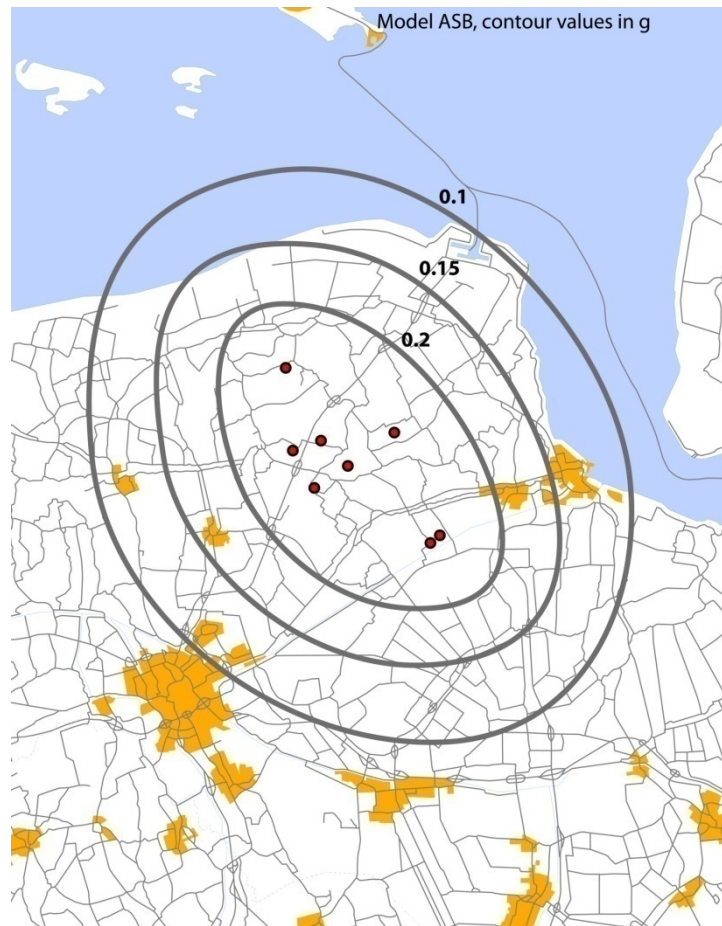


Figure 8. Contours for the highest median PGA due to a $M_w=5$ event in the area spanned by historical $M \geq 3$ events. Seismic sources are indicated as red circles, contours as grey lines. Median values are shown in g.

Both the PGV and PGA contours have been constructed using a $V_{s30} = 300$ m/s. Lowering this value to 200 m/s will increase the PGV value by 10% and decrease the PGA by approximately the same amount. The assumed style-of-faulting for the region is normal. In Figures 7 and 8 this means a maximum shift in the contours of ca 2 km and quantifies the uncertainty of the median value contours due to variations in the V_{s30} parameters. The maximum PGA value in Figure 8 is 0.26g. Lower and upper limits for the maximum PGA (median $\pm \sigma$) are: 0.13 g and 0.55 g.

In an integration of recent studies on seismic hazard of induced earthquakes in the Netherlands, Wassing and Dost (2012) provide an overview of soil categories in a site response map (Appendix 3, map 3). For the Groningen area two classes are of importance: “weak” soil ($V_{s30} \leq 200$ m/s) in the north-west of the Groningen gas field and “stiff” soil ($V_{s30} > 200$ m/s) to the south-east. Although only little information on measured V_{s30} in the region has been published, the contours shown in Figure 7 and 8 may provide a lower limit of the expected PGV and an upper limit for the PGA value in the region.

¹ 1 g = 981 cm/s^2

Probabilistic seismic hazard assessment (PSHA)

Van Eck et al. (2004, 2006) published a first probabilistic seismic hazard analysis (PSHA) for the Groningen field, based on recorded induced seismicity data for the period 1991-2003. The authors used the method originally proposed by Cornell (1968) and further developed by Cornell and Mertz (1975). In this method the probability of exceeding a specified ground motion at specific locations is calculated. The deterministic approach in the previous chapter provides specific scenarios, while the PSHA approach integrates over magnitude and distance, weighted by appropriate probability density functions.

The method requires characterization of the seismicity in the region and a proper attenuation relation (GMPE). An alternative method, based on a model relating gas production induced strain to earthquake activity was developed by Bourne & Oates (2013). Their PSHA calculations are based on a Monte Carlo simulation.

PSHA results will be used in a national guideline (NPR), currently in development by the Netherlands Standardization Institute (NEN), and later included in the national annex for Eurocode 8.

Seismicity

The dataset used by Van Eck et al. (2004, 2006) was limited to 54 events of $M_L \geq 1.5$ out of a total of 179 recorded events for the Groningen field. This dataset is now extended to 01-10-2013 and contains 195 events of $M_L > 1.5$. The classic PSHA method assumes seismicity to be a stationary Poisson process. In Groningen, however, the process is shown to be non-stationary.

Figure 10 shows the cumulative number of events and the annual number of events in the Groningen field per year. The cumulative number of events shows a linear trend in the log scale, which relates to an exponential growth. The annual number of events shows considerable fluctuations in time, as expected in a Poisson process. However, from 2003 on, a positive trend becomes apparent. Therefore, Dost and Kraaijpoel (2013) separated the database in two time intervals, 1991-2003 and 2003-2012. A comparison of the Gutenberg-Richter frequency-magnitude distribution calculated for the two time intervals showed that seismicity rate (a) increases with time and the b -value remains constant ($b=1.0 \pm 0.2$). In this analysis a bounded Gutenberg-Richter relation is assumed.

The fact that only the seismicity rate changes over time allows a conservative estimate of the hazard by extrapolating the seismicity rate to the end of the period assessed. It was decided to take a 5 year period: 2013-1018.

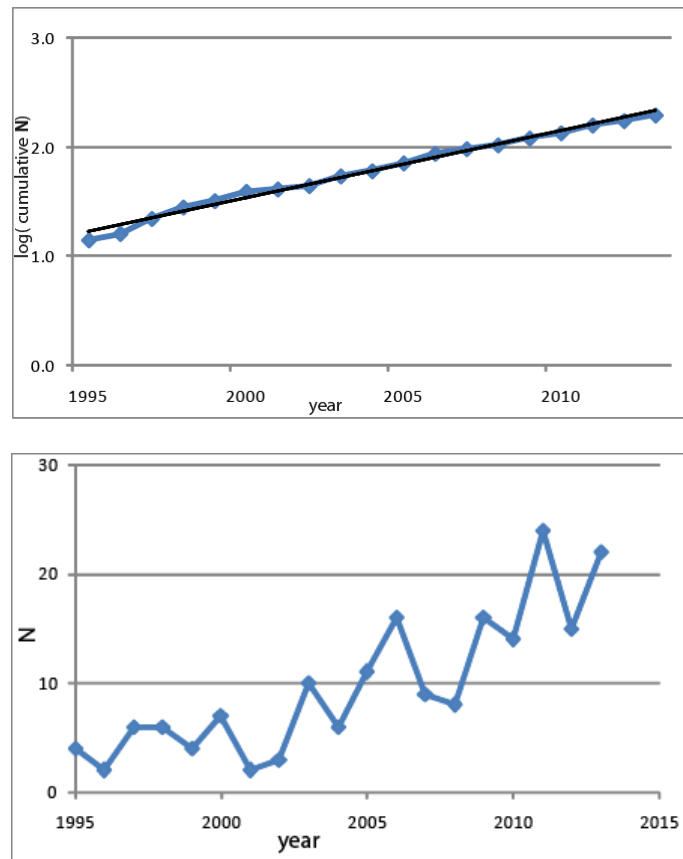


Figure 10. Upper: The logarithm of the cumulative number of events in the Groningen field and calculated trend for $M \geq 1.5$. Lower: annual number of events for $M \geq 1.5$. The seismicity dataset runs until October 1, 2013.

To forecast the annual number of events for 2018, we attempt linear fits to both the cumulative and annual numbers of recorded events (Figure 10). Fitting a linear trend to the logarithm of the cumulative annual number of events shows that this number will double in the next 5 years. A linear fit to both functions, starting at 2003, predicts for 2018 an average annual number of events of 26 and 33 respectively. Of course, this linear extrapolation depends on the production schedule for the coming years and possible other factors, so it is a first rough estimate.

At present the annual number of earthquakes of magnitude $M \geq 1.5$, the level of completeness for the region, is around 20. In the hazard evaluation we show results for an annual rate of 40 events.

Seismic source zones

Van Eck et al. (2006) used two source models for the Groningen field. The first one assumed the seismicity to be uniformly distributed over the gas field and the second assumed that seismicity is distributed over four identified main faults. The last ten years seismicity developed over a larger part of the field and shows a clear correlation with compaction.

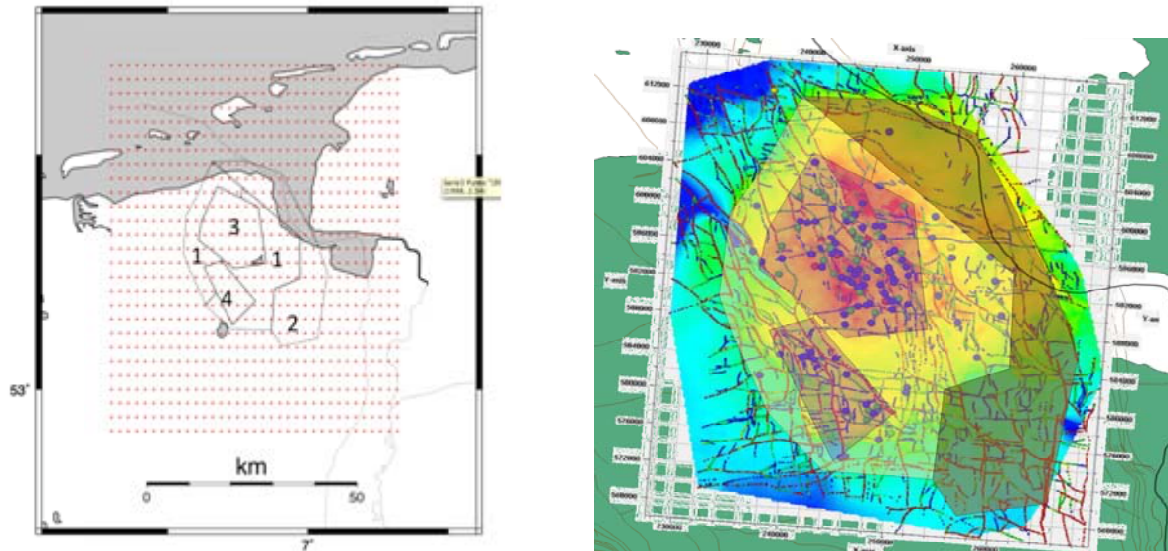


Figure 11. Left: Groningen gas field divided into source zones (1-4). Right: same source zones with information added on compaction (after Bourne & Oates (2013), red: >20cm), faults and seismicity.

Figure 11 shows the proposed definition of source zones for Groningen. Triggered events, which would be expected also at some distance to the field, are not considered. The most active zone (3) corresponds to the region of largest compaction and a high fault density. A large background zone (1) with more scattered seismicity is identified as second most active zone, followed by zone 4 and 2. An alternative classification can be introduced based on earthquake density instead of activity rate.

The assumed activity rate is distributed over the identified source zones using weights (table 2).

Background (1)	0.364
Eastern block (2)	0.017
Central north (3)	0.498
Central south (4)	0.121

Table 2: source zones and weights, based on the total number of events per zone since 1995

Maximum magnitude

A difficult parameter to estimate is the M_{\max} . Bourne & Oates (2013) discuss physical limits of the maximum magnitude, based on arguments with respect to the limit on finite strain, finite fault size and finite mass. The authors argue that if all strain accumulated over the life cycle of the field were released in one event at the end of production, the maximum magnitude is 6.5 for the Groningen field. Although this gives an absolute maximum, it is an unrealistic scenario, since many events have been recorded already and strain in elastic media that does not lead to failure is excluded. Until now only 0.1% of the total available strain energy is released in seismic energy. This value may increase with time, but we also assume that larger magnitude events require existing faults. The Groningen field is known to have many faults, but only a limited number of larger faults that may accommodate larger magnitude events.

Arguments based on a finite fault size provides an estimate of $M=5.8$ as a maximum value. However, this value corresponds to a slip of 0.3 m over a fault dimension of 3 km width and 60 km length. Since the part of the fault directly influenced by compaction is only 0.3 km, a more realistic estimate is a fault width of 1 km and a fault length of 20 km assuming a similar high aspect ratio of 20. This provides a $M=4.9$ and a slip of 0.1 m. In all calculations a stress drop of 1 MPa is assumed.

Finally, application of the relation between human made mass shifts and maximum magnitude from Klose (2013) to Groningen, with an estimated mass shift of 2.0 to 2.5 Gt, results in an expected maximum magnitude of around 4.5. However, Bourne & Oates (2013) argue that due to a substantial variation within the catalogue, a reasonable upper bound must be around 6. In his analysis Klose (2013) included larger magnitude events with $M>5$. In our view these events are triggered and not representative for the situation in Groningen, since there is no reported historical seismicity in the region and there is no evidence of events that have hypocenters far away from the gas producing layer.

There is some confusion on the interpretation of some of the events used by Klose (2013). The influence of larger tectonic events in the Pyrenees, located 20-30 km from the Lacq gas field and connected to the North Pyrenean Fault, was investigated by Grasso et al. (1992). The authors concluded that major regional events may trigger seismic instabilities in the vicinity of the gas extraction. This did not imply that the regional events were induced or triggered. More recently, Bardainne et al. (2008) state explicitly that the Lacq seismicity is clearly not linked to the natural seismicity of the Pyrenean range recorded 30 km further to the south.

These estimates show a large variety of physical limits to the maximum magnitude. Under the assumption that only induced events may occur, no triggered events, there are in our opinion no convincing arguments based on the finite mass limit or finite fault size to adopt a maximum magnitude higher than $M=5$ in our analysis. The absolute maximum has a relatively small influence on the PSHA results and a comparison for different choices for M_{\max} will be given.

The assumed activity rate in the present calculations can be compared to activity rate in the model used by Bourne & Oates (2013). Following Kagan (2002) the annual occurrence rate of events (α) with moments in the interval $[M_1, M_x]$ can be related to the annual seismic moment rate \dot{M} through:

$$\dot{M} = \frac{\alpha M_0^{\beta} \beta}{1-\beta} M_x^{1-\beta} \quad [12]$$

with $\beta = (2/3)b$ and $M_x \gg M_1$. Equation 12 is derived for a truncated Gutenberg-Richter distribution. Kagan (2002) also gives equations for other distributions e.g. a tapered Gutenberg-Richter distribution.

Bourne & Oates (2013) give estimates for the expected annual total seismic moment release for the period 2013-2023. The median of this parameter for 2018 is estimated at $1.9 \cdot 10^{14}$ Nm and in 2023 at $2.7 \cdot 10^{14}$ Nm. Assuming $M_x = 5$, the calculated event rate equals 10 in 2018 and 14 in 2023. An alternative is to assume an annual occurrence rate of 40 and calculate the maximum magnitude M_x . This results in $M_x = 3.8$ and 4.1 respectively. In all calculations $M_0 = 1.5$ and $b = 1.0$.

It should be noted that due to the Pareto sum distribution, the values for the upper bound of the 95% confidence interval of the total annual seismic moment are a factor 100 higher. For 2018 this value is $1.3 \cdot 10^{16}$ Nm and the assumption of $M_{max} = 5$ leads to an annual occurrence rate of 643.

Other parameters

The preferred attenuation relation (GMPE) for the Groningen field is the modified ASB relation, as discussed earlier, including the proposed standard deviation.

Van Eck et al. (2004, 2006) showed PSHA results for return periods of 10 and 100 years. This value was chosen since the duration of gas production is usually limited to one or several decades only. Since results from the PSHA calculations will be used in the national annex for Eurocode 8, it was decided to show results for a return period of 475 years, or 10% probability of exceedance in 50 years.

Results

Figure 12 shows results in terms of PGA and PGV for a 10% probability in 50 years (return period 475 years). The maximum value for PGV is 16 cm/s and for PGA the maximum value is 0.42 g. Comparison with previous results by Van Eck et al. (2004, 2006) is difficult, since different return periods are used.

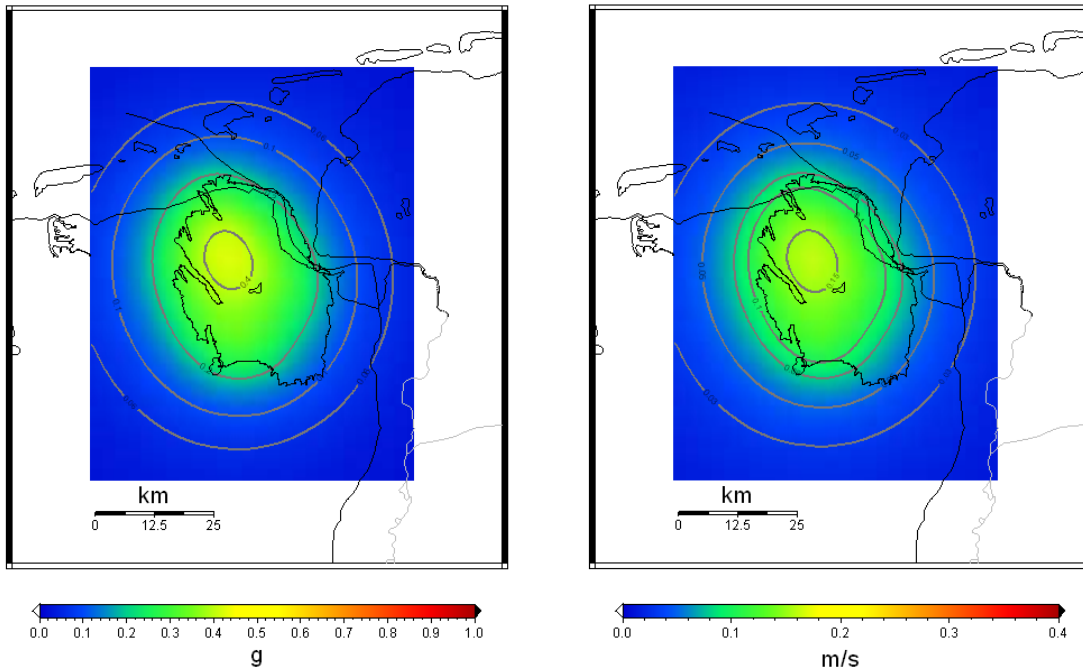


Figure 12. Estimated hazard around the Groningen field. Results for PGA (left, contour levels 0.05, 0.1, 0.2 and 0.4 g) and PGV (right, contour levels 0.03, 0.05, 0.07, 0.1 and 0.15 m/s) are shown for a return period of 475 year using the modified ASB13 model as GMPE and $M_{max}=5$.

The PGA hazard map for $M_{max}=5$ shows a small contour of $PGA=0.4g$ in the north-western part of the field. The small area of higher PGA values is possibly controlled by the chosen source area. The 0.2g contour spans most of the field area. For comparison results have been calculated for an assumed $M_{max}=6$. The maximum value for PGA increases to 0.50g and the PGV to 24 cm/s. This demonstrates the relative importance of the selected maximum magnitude.

The deterministic analysis provides one scenario for PGA and PGV, taking the median value of the GMPE used. The probabilistic results include the uncertainty in the GMPE and, as a result shows higher values. Both deterministic and probabilistic results are based on horizontal ground motions that dominate the seismic waveforms.

Further developments

The applicability of the selected GMPE for earthquakes of magnitude larger than 4 to Groningen is uncertain, although the model selected is the best available model. All GMPEs considered are empirical models, derived from measured acceleration data recorded in different tectonic settings. In case of Groningen the challenge is to extrapolate the calibrated part of the GMPE to higher magnitudes where no observations are available.

A solution is to calculate synthetic waveforms and to compare the predicted amplitudes at the surface to the empirical GMPEs. Therefore, it is recommended to investigate the influence of the local subsurface structure on the regional GMPE. The influence of a thick high velocity salt layer on top of the gas reservoir, which is the case in Groningen, was demonstrated to result in strong defocusing of seismic energy and in strong mode conversions (Kraaijpoel and Dost, 2013). Modelling the seismic wave field using a local velocity model will provide insight in the physics behind the empirical derived GMPEs and may be used to constrain the PGA and PGV values for events of magnitudes higher than so far recorded.

The results from the probabilistic seismic hazard analysis do include statistical uncertainties in the parameters used. Often we have limited knowledge on the parameters, e.g. for the M_{\max} or GMPEs, and we like to assess the influence of the lack of knowledge in these parameters (epistemic uncertainty) in the final results. It is recommended to investigate the influence of epistemic uncertainty in a logic-tree approach.

Conclusions

Evaluation of existing GMPEs and validation with acceleration data recorded during the Huizinge earthquake and 7 earlier events resulted in the creation of a reference GMPE for Groningen. Based on this relation and the assumption that the region where large events may occur is defined by past seismicity of $M \geq 3$, results of a deterministic hazard analysis are shown as contour maps of PGV and PGA for an $M=5$ event. These contour maps can be used as deterministic scenario's of what may happen during an earthquake of magnitude 5.

In addition to these deterministic scenarios also results of a probabilistic hazard analysis are presented. Results show contours of PGA and PGV values with a 10% chance in 50 years to be exceeded, or a return rate of 475 years which is commonly used in building-code guidelines. The presented results will be used in preparation for a national building-code guideline (NPR) and in the preparation of a national annex for Eurocode 8 for the Netherlands.

Uncertainties in the results presented are large, therefore research continues to further understand the influence of the subsurface in Groningen and to reduce these uncertainties.

Acknowledgements

Thanks to Julian Bommer for many stimulating discussions on this topic and for sharing his notes. Reviews by Julian Bommer and Torsten Dahm are much appreciated and greatly improved the report.

References

- Akkar, S., M.A. Sandikkaya and J.J. Bommer, 2013, Empirical Ground-Motion Models for Point- and Extended-Source Crustal Earthquake Scenarios in Europe and the Middle East, *Bulletin of Earthquake Engineering*, in press, DOI 10.1007/s10518-013-9461-4.
- Bardainne, T., N. Dubos-Sallee, G. Senechal, P. Gaillol and H. Perroud, 2008, Analysis of the induced seismicity of the Lacq gas field (Southwestern France) and model of deformation, *Geophysical Journal International*, **172**: 1151-1162
- Beyer, K. and J.J. Bommer, 2006, Relationships between median values and aleatory variabilities for different definitions of the horizontal component of motion. *Bulletin of the Seismological Society of America*, **94** (4A): 1512-1522.
- Bommer, J.J., P.J. Stafford, J.E. Alarcon & S. Akkar, 2007, The influence of magnitude range on empirical ground-motion prediction. *Bulletin of the Seismological Society of America*, **97**: 2152-2170.
- Bommer, J.J., J. Douglas, F. Scherbaum, F. Cotton, H. Bungum and D. Faeh, 2010, On the Selection of Ground-Motion Prediction Equations for Seismic Hazard Analysis, *Seismological Research Letters*, **81**: 783-793.
- Bommer, J.J. and S. Akkar, 2012, Consistent Source-to-Site Distance Metrics in Ground-Motion Prediction Equations and Seismic Source Models for PSHA. *Earthquake Spectra* **28**(1), 1-15.
- Bommer, J.J., 2013a, Seismic Hazard Assessment for Groningen Gas Field; Selection of Ground Motion Prediction Equation, *NAM Internal note* 30 pp.
- Bommer, J. J., 2013b, Proposals for New GMPEs for the Prediction of PGA and PGV in the Groningen Gas Field, *NAM internal note*, 37pp.
- Bourne, St. and S. Oates, 2013, Induced strain and induced earthquakes within the Groningen Gas Field: Earthquake probability estimates associated with future gas production, Rijswijk, the Netherlands, 68 pp.
- Cesca, S., T. Dahm, C. Juretzek and D. Kuehn, 2011, Rupture process of the 2001 May 7 Mw 4.3 Ekofisk induced earthquake, *Geophysical Journal International*, **187**: 407-413
- Chiou, B., R. Youngs, N. Abrahamson & K. Addo, 2010, Ground-motion attenuation model for small-to-moderate shallow crustal earthquakes in California and its implications on regionalization of ground-motion prediction models. *Earthquake Spectra* **26**(4), 907-926
- Cornell, C.A., 1968, Engineering seismic risk analysis, *Bulletin of the Seismological Society of America*, **58**: 1503-1606
- Cornell, C.A. and H.A. Mertz, 1975, Seismic risk analysis for Boston, *J. Structural Div.* **ST10**: 2027-2043
- Deichmann, N, 2006, Local magnitude, a moment revisited. *Bulletin of the Seismological Society of America*, **96**: 1267-1277.
- Dost, B., T. Van Eck and H. Haak, 2004, Scaling of peak ground acceleration and peak ground velocity recorded in the Netherlands, *Bolletino di Geofisica Teorica ed Applicata*, **45**(3): 153-168.

Dost, B. and H.W. Haak, 2007, Natural and induced seismicity, in Th. E. Wong, D.A.J. Batjes and J. de Jager, eds., *Geology of the Netherlands, Royal Netherlands Academy of Arts and Sciences*: 223-229.

Dost, B. and D. Kraaijpoel, 2013, The August 16, 2012 earthquake near Huizinge (Groningen), *KNMI report*, 26pp.

Douglas, J., B. Edwards, V. Convertito, N. Sharma, A. Tramelli, D. Kraaijpoel, B. M. Cabrera, N. Maercklin and C. Troise, 2013, Predicting Ground Motion from Induced Earthquakes in Geothermal Areas, *Bulletin of the Seismological Society of America*, **103**, doi: 10.1785/0120120197.

Grasso, J-R., J-P Gratier J.F. Gamond and J-C. Paumier, 1992, Stress transfer and seismic instabilities in the upper crust: example of the western Pyrenees, *Journal of Structural Geology*, **14**: 915-924.

Hanks, T. C. and D. M. Boore, 1984. Moment-magnitude relations in theory and practice, *Journal of Geophysical Research*, **89**: 6229-6235.

Kagan, Y.Y., 2002, Seismic moment distribution revisited: II. Moment conservation principle, *Geophysical Journal International*, **149**: 731-754.

Klose, C.D., 2013, Mechanical and statistical evidence of the causality of human-made mass shifts on the Earth's upper crust and the occurrence of earthquakes, *Journal of Seismology*, **17**: 109-135, DOI 10.1007/s10950-012-9321-8

Korff, M., H.M.G. Kruse, T.P. Stoutjesdijk, J. Breedveld, G.A. van den Ham, P. Holscher, G. de Lange, P. Meijers, E. Vastenburger, T. Vermaas and M.A.T. Visschedijk, 2013, Effecten geïnduceerde aardbevingen op kritische infrastructuur Groningen – Quick Scan naar de sterkte van de infrastructuur-, Deltares rapport, 87pp.

Kraaijpoel, D. and B. Dost, 2013, Implications of salt-related propagation and mode conversion effects on the analysis of induced seismicity, *Journal of Seismology* **17**: 95-107. DOI 10.1007/s10950-012-9309-4.

Muntendam, A.G. and J. A. de Waal, 2013, Reassessment of the probability of higher magnitude earthquakes in the Groningen gas field, Including a position statement by KNMI, *State Supervision of Mines report*, 35pp.

Van Eck, F. Goutbeek, H. Haak and B. Dost, 2004, Seismic hazard due to small shallow induced earthquakes, KNMI Scientific report; WR-2004-01, 52pp.

Van Eck, T., F. Goutbeek, H. Haak and B. Dost, 2006, Seismic hazard due to small-magnitude, shallow source, induced earthquakes in the Netherlands, *Engineering Geology*, **87**:105-121.

Van Eijs, R.M.H.E, F.M.M. Mulders, M. Nepveu, C.J. Kenter and B.C. Scheffers, 2006, Correlation between hydrocarbon reservoir properties and induced seismicity in the Netherlands, *Engineering Geology*, **84**: 99-111.

Wassing, B.B.T. and B. Dost, 2012, Seismische hazard van geïnduceerde aardbevingen; Integratie van deelstudies, *TNO/KNMI rapport (TNO 2012 R11139)*, 23pp.

Wells, D.L. and K.J. Coppersmith, 1994, New Empirical Relationships among Magnitude, Rupture Length, Rupture Width, Rupture Area, and Surface Displacement, *Bulletin of the Seismological Society of America*, **84** (4): 974-1002.